Accurate *ab initio* ro-vibronic spectroscopy of the $\tilde{X}^2\Pi$ CCN radical using explicitly correlated methods

J. Grant Hill,[(a)†] Alexander Mitrushchenkov,[(b)††] Kazim E. Yousaf,[(a)] and Kirk A. Peterson[(a)¶]

[(a)]*Department of Chemistry, Washington State University, Pullman, Washington 99164*

[(b)]*Université Paris-Est, Laboratoire Modélisation et Simulation Multi Echelle, MSME UMR 8208 CNRS, 5 bd Descartes, 77454 Marne la Vallée, France*

Abstract

Explicitly correlated CCSD(T)-F12b calculations have been carried out with systematic sequences of correlation consistent basis sets to determine accurate near-equilibrium potential energy surfaces for the $X^2\Pi$ and $a^4\Sigma^-$ electronic states of the CCN radical. After including contributions due to core correlation, scalar relativity, and higher order electron correlation effects, the latter utilizing large-scale multireference configuration interaction calculations, the resulting surfaces were employed in variational calculations of the ro-vibronic spectra. These calculations also included the use of accurate spin-orbit and dipole moment matrix elements. The resulting ro-vibronic transition energies, including the Renner-Teller subbands involving the bending mode, agree with the available experimental data to within 3 cm^{-1} in all cases. Full sets of spectroscopic constants are reported using the usual 2nd order perturbation theory expressions. Integrated absorption intensities are given for a number of selected vibronic band origins. A computational procedure similar to that used in the determination of the potential energy functions was also utilized to predict the formation enthalpy of CCN, $\Delta H_f(0K) = 161.7 \pm 0.5$ kcal/mol.

† Present address: School of Chemistry, Joseph Black Building, University of Glasgow, Glasgow G12 8QQ, UK; Electronic mail: grant.hill@glasgow.ac.uk

†† Electronic mail: Alexander.Mitrushchenkov@univ-mlv.fr

¶ Electronic mail: kipeters@wsu.edu

I. INTRODUCTION

The CCN radical should play an important role in reactions in the interstellar medium. As a proposed intermediate in the formation of larger cyano radicals this molecule may provide important insights into the development of interstellar clouds and other areas of extraterrestrial interest, such as star-forming regions. While the CN and C_3N radicals (and some larger cyano radicals with an odd number of carbon atoms) have been previously detected in the interstellar medium,[1] CCN has yet to be observed by radioastronomy. Efforts are hampered by the $^2\Pi$ electronic ground state of CCN possessing a small electric dipole moment,[2] which is around seven times smaller than the equivalent dipole in the $^2\Sigma^+$ ground state of C_3N.[3,4] A density functional theory study on the formation of CCN found the process to be strongly endothermic, suggesting that the radical cannot be synthesized in cold molecular clouds but may be found in much warmer circumstellar envelopes.[5] While the same theoretical study identified IRC+10216 as a potential candidate, an extensive search towards this circumstellar gas led to a negative result.[6] It is interesting to note that the phosphorous containing dicarbide analog CCP, which has a much larger dipole moment, has been detected in this same region of space, implying that CCN may be detected if more sensitive observations are carried out.[7]

Chemical interest in CCN is not limited to the interstellar medium, since as a linear system with a $^2\Pi$ electronic ground state there are degenerate $^2A'$ and $^2A''$ states resulting in a strong Renner-Teller effect on the bending modes. The CCN radical was first observed in 1965 *via* flash photolysis of diazoacetonitrile.[8] Further experiments have since refined the spectroscopic constants for the $^2\Pi$ electronic ground state,[9,10-14] while theoretical studies have probed *ab initio* spectroscopy, thermochemistry and reactivity.[3,5,15,16-18] In particular relevance to the current investigation, Pd and Chandra[3] optimized the $X^2\Pi$ geometry at the full valence space complete active space self-consistent field (CASSCF) level with a well-tempered Huzinaga basis set[19] augmented with additional polarization functions taken from the density matrix averaged atomic natural orbital (ANO) basis sets.[20] Harmonic frequencies were obtained at the same level of theory using numerical Hessians, with the Renner parameter computed to be 0.483, which can be compared to an experimentally derived value of 0.42.[11,12] Single point total electronic energies were then obtained at the multireference singles and doubles configuration interaction level. Rosmus and co-workers[18] reported the ro-vibronic spectrum of the $^2\Pi_{1/2}$ ground state of CCN calculated using a near-equilibrium potential energy function obtained at the CASSCF level of

theory. With a variational treatment of the Renner-Teller effect including spin-orbit coupling, they were able to reproduce the known ro-vibronic transitions to within 10-20 cm^{-1} with small empirical adjustments to the quadratic portion of their PES. In a related study, an internally contracted multireference configuration interaction (icMRCI) study, including the Davidson correction (+Q), of the isoelectronic CCO^+ radical was recently carried out with the cc-pV5Z basis set by Jutier and Léonard.[21] These calculations confirmed that CCO^+ has a $^2\Pi$ ground state with a low lying $a^4\Sigma^-$ excited state that is 2388 cm^{-1} higher in energy. As this radical is isoelectronic with CCN, a similar excited state may also be important to the spectroscopy of the present investigation, especially in terms of its interaction via spin-orbit coupling. The MRCI calculations (including zero point correction) of Pd and Chandra[3] predicted the $a^4\Sigma^-$ state to be 8322 cm^{-1} higher than the ground state for CCN, which is in good agreement with the recent observation of this state by slow photoelectron velocity-map imaging spectroscopy by Neumark and co-workers,[22] $T_0 = 8413 \pm 8$ cm^{-1}.

The slow convergence of correlated *ab initio* methods with respect to basis set size is well known, with the obvious consequence that the calculation of high-accuracy spectroscopy becomes computationally expensive, even for small gas phase molecules. Over the last decade a large amount of effort has been focused on the development of new theoretical methods that include terms depending explicitly on the interelectronic distance. Recent review articles[23] cover these developments in depth, including examples of how the basis set dependence of these methods are greatly reduced compared to their conventional analogues, while requiring only a modest increase in computer time. In the present work, it will be demonstrated that the explicitly correlated coupled cluster with singles, doubles and perturbative triples, CCSD(T)-F12b, method[24] can produce a highly accurate potential energy surface (PES) for CCN with relatively moderate basis set requirements. A composite approach is taken to correct the PES for the effects of core-valence correlation, scalar relativistic effects, and higher order correlation. Composite PESs for both components of the $X^2\Pi$ as well as the excited $a^4\Sigma^-$ state are then combined with accurate dipole moment and spin-orbit functions in variational nuclear motion calculations to produce spectroscopic constants that are in excellent agreement with the available experimental data.

II. METHODOLOGY

A. Determination of the potential energy surfaces

Unless stated otherwise, all electronic structure calculations were carried out with the MOLPRO[25] package of *ab initio* programs. Near-equilibrium potential energy surfaces for both the ^{2}A′ and ^{2}A″ components of the degenerate X$^2\Pi$ ground state of CCN, as well as the $a^4\Sigma^-$ excited state, were calculated from 50 symmetry-unique points around near-equilibrium geometries, these points lying in the range $-0.3a_0 < \Delta R < 0.5a_0$ for $\Delta R = R - R_e$ in the distances between two adjacent atoms and $150° \le \theta \le 180°$ for the included angle between the atoms. The total energy, E, at each geometry was obtained in a composite manner, such that:

$$E(r_1, r_2, \theta) = \text{CCSD(T)/CBS} + \Delta\text{CV} + \Delta\text{DK} + \Delta\text{HC} \quad (1)$$

where CCSD(T)/CBS is an estimate of the complete basis set (CBS) limit obtained within the frozen core approximation at the coupled cluster singles and doubles level of theory with perturbative triples, ΔCV is a correction for the effects of 1*s* electron correlation, ΔDK is a correction for scalar relativistic effects, and ΔHC estimates the total effect of higher level electron correlation beyond CCSD(T).

The frozen-core CCSD(T) total energies were obtained with the explicitly correlated R/UCCSD(T)-F12b method[24] using the 3C(FIX) diagonal, fixed amplitude *ansatz*.[26] This implementation is spin unrestricted in the CCSD equations but employs restricted open shell HF (ROHF) orbitals.[27] The orbital basis sets for all atoms corresponded to the correlation consistent cc-pV*n*Z-F12 (*n* = D, T, Q) sets,[28] with the cc-pV*n*Z/JKFIT[29] auxiliary basis sets (ABSs) utilized in the density fitting of the Fock and exchange matrices[30] (except that cc-pVTZ/JKFIT was used in combination with the cc-pVDZ-F12 orbital basis). The aug-cc-pV*n*Z/MP2FIT[31] ABSs were used in the density fitting of the remaining two-electron integrals, and the cc-pV*n*Z-F12/OPTRI[32] ABSs were used in the resolution of the identity (RI).[33] The latter was performed following the complementary auxiliary basis set (CABS) protocol,[34] as implemented in MOLPRO.[35,36] The values of the geminal Slater exponent, γ, were set to 0.9 for cc-pVDZ-F12 and 1.0 a_0^{-1} for the remaining orbital sets, as recommended elsewhere for the given combinations of basis sets.[37] The resulting CCSD and (T) components of the correlation energy were each individually extrapolated towards the CBS limit using a Schwenke-style[38] approach:

$$E_{CBS}^{corr} = (E_{VQZ}^{corr} - E_{VTZ}^{corr})F + E_{VTZ}^{corr} \quad (2)$$

where F is a coefficient that has been previously optimized[37] to reproduce accurate estimates of the correlation energy components for a set of small molecules, given a specific pair of basis sets with the CCSD(T)-F12b method (for TZ/QZ F = 1.363388 for the CCSD-F12b correlation energy and 1.769474 for the (T) contribution). The total energy is then formed from the sum of these two extrapolated values added to the ROHF/cc-pVQZ-F12 energy, where the latter also included a CABS singles correction.[36]

The corrections for core-valence correlation were obtained from CCSD(T)-F12b calculations with all electrons correlated, using the cc-pCVTZ-F12 orbital basis set[39] along with cc-pCVTZ-F12/OPTRI,[39] cc-pVTZ/JKFIT, and aug-cc-pwCVTZ/MP2FIT[40] ABSs. The net core-valence correction, ΔCV, was evaluated as $E_{core+val} - E_{val}$, where $E_{core+val}$ is the CCSD(T)-F12b/cc-pCVTZ-F12 total energy with all electrons correlated and E_{val} is the CCSD(T)-F12b/cc-pCVTZ-F12 total energy within the frozen core approximation. A γ value of 1.4 a_0^{-1}, as recommended for obtaining core-valence effects at this level of theory,[39] was used in both cases.

The corrections for scalar relativistic effects at each geometry were calculated as $\Delta DK = E_{DK2} - E_{NR}$ where E_{DK2} is the total second-order Douglas-Kroll-Hess (DKH)[41] R/UCCSD(T) energy using the cc-pVTZ-DK basis set,[42] and E_{NR} is the non-relativistic R/UCCSD(T) total energy in the standard cc-pVTZ basis.[43]

The effects of higher level electron correlation beyond the CCSD(T) level of theory, ΔHC, were calculated in two different ways. The initial approach utilized high order coupled cluster theory, which is typically the approach in accurate *ab initio* thermochemistry schemes[44,45]:

$$\Delta HC = \Delta T + \Delta Q + \Delta FCI(cf)$$

The contribution of the effects of iterative triple excitations was defined as $\Delta T = E_{CCSDT} - E_{CCSD(T)}$, where both the ROHF-based CCSD(T) and CCSDT[46] total energies were calculated with the cc-pVTZ basis set[43] within the frozen-core approximation, with the CCSDT calculations employing the MRCC program[47] interfaced to MOLPRO. Similarly, the correction for connected quadruple excitations was obtained as $\Delta Q = E_{CCSDTQ} - E_{CCSDT}$ with the cc-pVDZ basis set,[43] also with the MRCC program. An estimate of the difference in correlation energy between CCSDTQ[48] and full CI (FCI) was obtained by carrying out continued fraction (*cf*) extrapolations[49] from the CCSD, CCSDT, and CCSDTQ total energies evaluated with the cc-pVDZ basis set. This extrapolation is defined as:

$$E_{FCI(cf)} = \frac{E_{CCSD}}{1 - \frac{\left(\frac{\delta_T}{E_{CCSD}}\right)}{\left(1 - \frac{\delta_Q}{\delta_T}\right)}} \tag{3}$$

where $\delta_T = E(\text{CCSDT}) - E(\text{CCSD})$ and $\delta_Q = E(\text{CCSDTQ}) - E(\text{CCSDT})$. Therefore the ΔFCI correction can be expressed as $\Delta FCI(cf) = E_{FCI(cf)} - E_{CCSDTQ}$. While this correction should be treated with some skepticism, it has been previously shown to yield reliable estimates of the FCI correlation energy limit in many cases.[44] We also investigated an alternative *cf* extrapolation whereby only the CCSD correlation energy was used in Eq. (3) rather than the total energy. In this case $\Delta FCI(cf, corr) = E^{corr}_{FCI(cf)} - E^{corr}_{CCSDTQ}$. For both the $^2\Pi$ and $^4\Sigma^-$ states these higher order correlation corrections were essential for obtaining accurate results (see below), as might have been expected from the relatively large T_1 diagnostics[50] of 0.032 and 0.041, respectively, (D_1 diagnostics[51] both ~0.08) in the CCSD calculations near their equilibrium geometries. It should also be noted that while CCSDTQP calculations would be preferable to such an extrapolation scheme, the computational expense to calculate this correction for a total of 150 geometries (50 points on each PES) would have been prohibitive with current available resources.

As an alternative to the coupled cluster approach to ΔHC as described above, which unfortunately is limited to only very small basis sets (cc-pVDZ) due to the computational cost of the CCSDTQ calculations, internally contracted multireference configuration interaction (icMRCI) calculations[52] with single and double excitations were also carried out with the cc-pVTZ basis set. These employed CASSCF orbitals with full valence active spaces (~170,000 configuration state functions in C_s symmetry) where only the 1*s* orbitals of C and N were constrained to be doubly occupied in all configurations. In the cases of the ^{2}A′ and ^{2}A″ states, the orbitals were also state averaged with equal weights. This same full valence active space was then used as the reference function in subsequent frozen-core icMRCI calculations, yielding 22–23 million variational parameters in C_s symmetry (corresponding to about 1.4 billion uncontracted). The resulting higher level correlation correction based on these MRCI calculations at each geometry was then defined as $\Delta\text{MRCI} = E(\text{icMRCI}) - E(\text{CCSD(T)})$. The inclusion of a multireference Davidson correction[53] (+Q) was also investigated, leading to

$\Delta\text{MRCI+Q} = E(\text{icMRCI+Q}) - E(\text{CCSD(T)})$. Of course the CCSD(T) calculations in these cases also used the cc-pVTZ basis set.

The various grids of 50 energies corresponding to Eq. (1) were fit to polynomial functions of the form

$$V(Q_1,Q_2,Q_3) = \sum_{ijk} C_{ijk} (Q_1)^i (Q_2)^j (Q_3)^k \qquad (4)$$

to represent the individual potential energy surfaces at each level of approximation. The coordinate Q_1 in Eq. (4) corresponds to the CC internuclear distance, Q_2 represents the CN distance, and Q_3 is the CCN valence angle. The summation included a full set of quartic with some selected quintic- and sextic-order coefficients with typical root-mean-square (RMS) errors in the fits of less than 0.3 cm^{-1} with maximum errors of about 1 cm^{-1} or less for the $^2\Pi$ state. The analogous fitting errors for the $^4\Sigma^-$ state were slightly larger at 1.2 and 3.2 cm^{-1}, respectively. To improve the asymptotic behavior of the resulting surfaces, Morse-like coordinates, $Q_i = \left[1 - e^{-\beta_i (r_i - r_{i,e})/r_{i,e}}\right] \Big/ \beta_i$, were used for both stretching coordinates with the Morse parameters β_i roughly optimized. The final $^2\Pi$ state PES used in the variational calculations of the ro-vibronic spectrum employed separate fits to the average, $V_+ = (A' + A'')/2$, and the difference, $V_- = (A' - A'')/2$, PESs. These expansion coefficients, together with those for the $^4\Sigma^-$ state, are explicitly given in Table S1 of the supplemental material.[54] Quartic internal coordinate force fields for each state are given in Table S2. The fitting of the surfaces and subsequent second-order perturbation theory calculations[55] of the spectroscopic constants were carried out with the SURFIT program.[56]

B. Variational nuclear motion calculations of the ro-vibronic spectrum

The calculation of the ro-vibronic spectrum for the $X^2\Pi$ state of CCN involved three potential energy surfaces (both components of the $^2\Pi$ as well as the $^4\Sigma^-$), permanent and transition dipole moment functions for both components of the $^2\Pi$, and spin-orbit coupling matrix elements between all 3 states.

The permanent electric dipole moments for both the $^2A'$ and $^2A''$ components of the $X^2\Pi$ state were calculated at the same 50 points as the PES at the R/UCCSD(T) level of theory with

the aug-cc-pVTZ basis set[57] by applying finite fields (± 0.002 a.u.) to the one-electron Hamiltonian. The transition dipole moments between the ^{2}A′ and ^{2}A″ states were calculated as expectation values at each grid point using the state-averaged, full valence CASSCF level of theory, also with the aug-cc-pVTZ basis. Analytical permanent and transition dipole moment functions were obtained by employing quartic polynomial fits analogous to Eq. (4), but using simple displacement coordinates throughout, e.g., $Q_1 = r_1 - r_{1,e}$. The expansion coefficients are given in Table S3.

Spin-orbit coupling matrix elements were also calculated at the full valence space, state-averaged CASSCF level of theory at each grid point. The unique matrix elements connecting the ^{2}A′, ^{2}A″ , and $^4\Sigma^-$ (^{4}A″ in C_s) electronic states were obtained using the full Breit-Pauli spin-orbit operator.[58] The basis set employed consisted of the contracted *s* and *p* functions from the cc-pCVQZ basis set,[59] the *d* functions from the cc-pVQZ basis,[43] and additional tight *p* functions (294.6, 54.91 a_o^{-2} for C and 406.1, 87.59 a_o^{-2} for N) as recommended by Nicklass *et al*.[60] The resulting unique spin-orbit matrix elements,

$\left\langle {}^2A' \middle| LS_y \middle| {}^2A'' \right\rangle, i\left\langle {}^2A' \middle| LS_z \middle| {}^2A'' \right\rangle, i\left\langle {}^2A'' \middle| LS_x \middle| {}^4\Sigma^- \right\rangle, \left\langle {}^2A' \middle| LS_y \middle| {}^4\Sigma^- \right\rangle$, and $i\left\langle {}^2A' \middle| LS_z \middle| {}^4\Sigma^- \right\rangle$

were then fit in the same manner as the dipole moments with expansion coefficients given in Table S4.

Finally, for the Renner-Teller vibronic treatment the $L_{x,y}$ operators and the geometry variations of the expectation values of the L_z, and L_z^2 operators have been neglected. The expectation values of the L_z and L_z^2 operators were set to unity.

To calculate ro-vibronic levels and transition intensities, the recently developed EVEREST code[61] has been used. This program uses the exact nuclear kinetic energy operator for triatomic molecules $\hat{K}_K$ as in, e.g., Ref. 62. Here the index *K* is the projection of the rotational angular momentum $-\mathbf{L}$ on the molecule fixed *z*-axis (see Sec. III.C.1 below). One should note the negative sign of the molecule-fixed definition,[62] which insures the standard commutation relations of angular momentum operator are obeyed. The Sutcliffe-Tennyson Hamiltonian[62] was generalized to the case of coupled Renner-Teller states. As shown in Ref. 63, this is done by writing the vibronic part of the wave function as a linear combination of two Renner-Teller components

$$\phi_K(r_1,r_2,\theta,y)=\frac{1}{r_1r_2}\left\{\left|+\Lambda\right\rangle\chi_+(r_1,r_2,\theta)\ +\ \left|-\Lambda\right\rangle\chi_-(r_1,r_2,\theta)\right\}$$

where r_1, r_2, and θ are internal coordinates, y is a set of electronic coordinates in the molecule-fixed frame, and the electronic components with a given z-projection Λ at linear geometries of electronic angular momentum $\mathbf{L}_{eq}$ in the molecule-fixed frame are defined as $\left|\pm\Lambda\right\rangle=\frac{1}{\sqrt{2}}\left(\left|A'\right\rangle\pm i\left|A''\right\rangle\right)$. Then as was shown in Ref. 63, the nuclear kinetic energy is the same as for non-degenerate electronic states but with $\mathbf{L}$ (denoted as $\mathbf{\Pi}$ in Ref. 63) replaced with $\mathbf{L}+\mathbf{L}_{eq}$ ($\mathbf{L}_{eq}$ is denoted $\mathbf{L}$ in Ref. 63). Then for a pair of functions $\left\{\chi_+,\chi_-\right\}$, the vibrational Hamiltonian becomes a 2x2 matrix given by

$$\delta_{K'K}\begin{pmatrix}\hat{K}_{|K-\Lambda|}+V_+ & V_-\\ V_- & \hat{K}_{|K+\Lambda|}+V_+\end{pmatrix}$$

where

$$V_\pm=\frac{1}{2}(V_{A'}\pm V_{A''})$$

The operator $\hat{K}_K$ is still given as a sum of three terms, Eqs.(28, 29, 31) of Ref. 62. For K=0, the kinetic energy operators are identical and the vibrational Hamiltonian can be back-transformed to the $\left\{A',A''\right\}$ basis, completely decoupling electronic and vibrational degrees of freedom; in this case the equations are similar to those of non-degenerate electronic states. The rotation-free vibronic equation was solved by diagonalizing the vibrational Hamiltonian for all $0\le K\le 20$. Bond-lengths/bond-angle coordinates are used throughout. In fact, for such coordinates the Hamiltonian operator is identical to that of Ref. 63. As basis functions, products of 120 normalized associated Legendre functions and 60 Sinc-DVR[64] functions for each bond were used. The Sinc-DVR functions were built on the interval [1.9...5.4] bohr for the C-C bond and on the interval [1.8...4.0] bohr for the C-N bond. No contraction of the basis set was used and a full 3-dimensional diagonalization was performed using a Jacobi-Davidson algorithm.[65] These calculations included vibrational states up to 7000 cm^{-1} above the (000) level of the $X^2\Pi$ state and up to 4000 cm^{-1} above the (000) level for the $a^4\Sigma^-$ state. The resulting vibronic states were then used to perform a full ro-vibrational diagonalization, including now also all rotational $\hat{K}_{VR}$

terms. The operators λ (Ref. 62) were modified to the Renner-Teller case similar to the vibrational Hamiltonian, i.e., by replacing index K by $K \mp \Lambda$. Also at this stage the spin-orbit interaction was accounted for. For spin-dependent interactions it was preferable to use the Hund's case *b* coupling scheme by writing basis functions as

$$\left|JM_J NKIi\right\rangle = \sum_{M M_S} C^{JM_J}_{NMS_I M_S} \left|NMKIi\right\rangle \left|S_I M_S\right\rangle$$

where C are the Clebsch-Gordan coefficients, $\left|NMKIi\right\rangle$ are the spin-free basis functions with total angular momentum N and its projections to laboratory- and molecule-fixed axes M and K, respectively. Indices I and i correspond to the electronic and vibrational state, respectively. Finally, $\left|S_I M_S\right\rangle$ are the spin functions with S_I being the electronic spin of the I-th state along with its projection onto the laboratory frame z-axis, M_S. The advantage of using the Hund's case *b* scheme is that all spin-free operators, as kinetic energy and electronic potentials, are diagonal and independent of J, and thus have exactly the same expressions as in the spin-free case. The matrix elements of the spin-orbit interaction can be easily written in such a basis by using general angular momentum theory expressions. The full details of the Hamiltonian expressions and a complete description of the EVEREST code will be given elsewhere.[61]

Rotational diagonalizations were carried out with J up to 155/2. The dipole moment surfaces were then used to evaluate the ro-vibrational transition matrix elements and generate the synthetic spectra, as in, e.g. Ref. 66. In a similar fashion, this EVEREST code has been previously applied to the vibronic spectrum of the HS_2 molecule.[67]

III. RESULTS

A. The $X^2\Pi$ state

Table I shows the equilibrium bond lengths, anharmonic frequencies (calculated *via* SURFIT), and total equilibrium atomization energies (ΣD_e) for the $X^2\Pi$ CCN radical, where the $\left({}^2A' + {}^2A''\right)/2$ average PES was used for these results. The convergence with respect to the basis set at the CCSD(T)-F12b level is observed to be very rapid, as one may expect from an explicitly correlated method. Even on going from the small double-ζ to the triple-ζ basis set, the bond lengths change by only one or two thousandths of an angstrom. Extrapolation to the CBS limit produces only minor changes in bond lengths and anharmonic frequencies compared to the cc-

pVQZ-F12 values, and the ΣD_e is increased by only 0.4 kcal/mol. The convergence of the harmonic frequencies with basis set are plotted in Figure 1, where the CBS limit values are indicated by the dashed line. It can be seen that ω_1 (CN stretch) converges at a significantly slower rate than the other two modes, which is presumably due to its multiple bond character. In all cases convergence towards the limit is smooth and the cc-pVQZ-F12 frequencies are only a few tenths of a cm^{-1} from those at the estimated CBS limit.

Correlating the 1*s* electrons results in a decrease of the C-C and C-N bond lengths by 0.0038 and 0.0026 Å, respectively, compared to the frozen-core values. Core correlation also produces increases in the vibrational frequencies as large as 9 cm^{-1} and increases the ΣD_e by 1.7 kcal/mol. The correction for scalar relativistic effects was very small, as might be expected for such light atoms, but appears to be necessary to approach wavenumber accuracy in the anharmonic frequencies.

Upon comparison to the available experimental values, the CCSD(T)/CBS + ΔCV + ΔDK level of theory still yields a CN stretching frequency (ν_1) that is too large by about 18 cm^{-1}. Hence electron correlation effects beyond CCSD(T) would certainly seem to be required in this case for high accuracy. Employing the difference between MRCI+Q and CCSD(T) with the cc-pVTZ basis set at each point, denoted ΔMRCI+Q in Table I, yields excellent agreement with experiment[10] for both the CN and CC stretching fundamentals. It should be noted that the analogous correction without the +Q correction, ΔMRCI, has a smaller overall effect, especially for the CN stretching frequency. The CCSD(T)/CBS+ΔCV+ΔDK+ΔMRCI+Q level represents the final, composite PES for $X^2\Pi$ CCN used in all further calculations below.

For the sake of comparison, results using surfaces employing higher level correlation corrections obtained by coupled cluster theory are also shown in Table I. Effects from including the difference between CCSD(T) and CCSDT, i.e., ΔT, are observed to be generally small, although υ_1 is observed to increase by almost 6 cm^{-1} (away from the experimental value). Inclusion of full iterative quadruples (CCSDTQ - CCSDT), however, is more substantial and reduces the C-C bond length by 0.001 Å, increases the C-N bond length by 0.0023 Å, and decreases the CN stretching frequency (ν_1) by more than 15 cm^{-1}. With such a large effect resulting from connected quadruple excitations, it might be expected that even higher level electron correlation, e.g., CCSDTQP, might be required for the CN stretching mode. Unfortunately these calculations are out of reach for CCN and one has to rely upon schemes like

the continued fraction (*cf*) extrapolation to improve the PES. If the *cf* extrapolation is carried out in the typical manner using the CCSD total energy with the CCSDT and CCSDTQ increments, denoted ΔFCI(cf), the resulting frequencies are not significantly improved, e.g., ν_1 is further decreased by just 3 cm^{-1} and is still larger than experiment by about 5 cm^{-1}. The convergence of the harmonic frequencies with the coupled cluster excitation level (CCSD, CCSDT, CCSDTQ), all in the cc-pVDZ basis set, is shown in Figure 2. Just as in the case of the basis set convergence, the convergence of ω_1 is noticeably slower than the other modes. All of the modes, however, seem to converge smoothly towards the FCI(cf) result. On the other hand, as also shown in Table I, if the *cf* extrapolation is based on the CCSD correlation energy, the resulting ΔFCI(cf,corr) correction seems to be much too large, decreasing the CN stretching fundamental by nearly 20 cm^{-1} and strongly overshooting the experimental value. Based on these results, use of the coupled cluster sequence with FCI(cf) yields reasonable estimates of the effects of higher level electron correlation, but the most accurate treatment for CCN, at least for the near-equilibrium spectroscopic properties, appears to be obtained at the MRCI+Q/cc-pVTZ level of theory. The poorer agreement with experiment when using the coupled cluster based methods is presumably due to the limitation of using just a cc-pVDZ basis set for CCSDTQ, as well as the inability to explicitly carry out CCSDTQP (and higher) calculations.

Spectroscopic constants calculated by second order perturbation theory from the final composite potential energy function given in Table S1 are shown in Table II. The predicted equilibrium bond lengths are expected to be accurate to under 0.001 Å. Upon comparison to previous *ab initio* calculations, only the CC distance appears to be strongly sensitive to the level of theory. The previous CASSCF value of Pd and Chandra,[3] as well as the SAC-CI result of Ehara *et al.*,[17] are too long by ~0.03 Å, except for the older CASSCF value of Gabriel *et al.*[18] where the two lowest σ orbitals were constrained to be doubly occupied in the active space. The all-electrons correlated, CCSD(T)/TZ2P result of Martin *et al.*[16] is in fair agreement with the current results, but their CC distance is still too long by about 0.015 Å. The ground state rotational constant (B_0) calculated on the averaged PES of this work differs from the experimental value of Allen *et al.*[11] (11,933.790 MHz) by just under 10 MHz. Comparison of the *ab initio* harmonic frequencies calculated in the current investigation and those derived in the experimental work of Oliphant *et al.*[10] (ω_1 = 1930.7, ω_2 = 324.0, ω_3 = 1045.9 cm^{-1}) do not show very good agreement, even though the three anharmonicity constants they were able to include (in cm^{-1}: X_{12} = -7.489, X_{23} = 11.536, and X_{33} = -2.600) are actually quite close to those of the

present work. Sufficient experimental data to determine a complete set of anharmonicity constants was not available and this evidently strongly affects the accuracy of the resulting harmonic frequencies since the anharmonic band origins of the present work are in excellent agreement with experiment. In particular, as shown in Table II both X_{11} and X_{13} are large and non-negligible. The latter are in good agreement with the older experimental work of Hakuta and Uehara.[13]

The splitting of the degeneracy between the ^{2}A′ and ^{2}A″ states upon bending is shown in Figure 3 as a cut of the PES through the bending angle with the bond lengths fixed at their equilibrium values. The two states separate strongly with deviations from linearity, resulting in a difference in the two harmonic frequencies of ~140 cm^{-1} and a relatively large value of the Renner parameter ε of 0.429. The latter is in very good agreement with the experimental value derived by Allen *et al*.,[11] 0.42. It can also be seen that the ^{2}A″ state is lower in energy as the molecule bends away from linear. Experimentally the value of $\varepsilon\omega_2$ was reported as 134.84 cm^{-1} by Beaton *et al*.[12] from a revised fit of the data of Allen *et al*.[11] The Beaton *et al*. value differs by only ~3 cm^{-1} from the *ab initio* result shown in Table II.

B. The $a^4\Sigma^-$ state

As detailed above, a potential energy surface was also obtained for the $a^4\Sigma^-$ excited state of CCN using the same composite method, and the coefficients from Eq. (1) defining the PES are also given in Table S1. The convergence of the equilibrium bond lengths and anharmonic frequencies with respect to basis set and method is presented in Table III. Just as in the ground state case, convergence with respect to basis set is rapid, and the values calculated on the estimated CBS limit PES are very close to the F12 results produced with the cc-pVQZ-F12 basis set. The effects of the remaining parts of the composite scheme are also analogous to that seen in Table I for the ground state. Correlating the 1*s* electrons decreases the C-C and C-N bond lengths by 0.0032 and 0.0026 Å, respectively, while scalar relativistic effects are very small. Similar to the ground state (Table I), the higher order correlation correction based on icMRCI+Q calculations (ΔMRCI+Q) is in fair agreement with the ΔFCI(cf) results, with the CN stretching frequency exhibiting the largest difference. As in the ground state the inclusion of full iterative quadruples also has a noticeably larger effect than the difference between CCSDT and CCSD(T). The energy difference between the equilibrium structure of this excited state and that of the

ground state is 24.12 kcal/mol (8435 cm^{-1}) which is a much larger separation than in the isoelectronic CCO^+ molecule[21] and in good agreement with the MRD-CI value previously calculated by Pd and Chandra.[3] The adiabatic state separation T_0 is shown in Table III and is predicted to be 8544 cm^{-1} after all corrections are included. This is slightly higher than the recent experimental value of Garand et al.,[22] 8413 ± 8 cm^{-1}. Hence, at least for this state separation, the higher order correlation correction calculated at the MRCI+Q level (+270 cm^{-1}) is somewhat too large while the ΔHC correction based on coupled cluster theory (+77 cm^{-1}) is much smaller and leads to better agreement with experiment. In contrast, the difference between ΔHC values for the bond lengths and vibrational band origins are more similar to the ground state results shown in Table I, where the ΔMRCI+Q corrections were observed to be the most accurate. A full set of spectroscopic constants calculated via second order perturbation theory for the $a^4\Sigma^-$ excited state using the CCSD(T)/CBS+ΔCV+ΔDK+ΔMRCI+Q PES are given in Table IV. As compared to previous calculations in the literature,[3,16,22] the agreement with the present equilibrium bond lengths follows the same general trends as the ground state. In addition the coupled cluster harmonic frequencies reported by Martin *et al*.[16] are in much better agreement with the present results than the CASSCF values of Pd and Chandra.[3] Last, the calculated value for the ν_3 fundamental, 1175.4 cm^{-1}, is within the uncertainty of the experimental value of Garand et al.,[22] 1170 ± 8 cm^{-1} (assuming the experimental uncertainty in this frequency is the same as that of the adiabatic state separation).

C. Variational calculation of the ro-vibronic spectrum of CCN

1. Ro-vibronic structure

The ro-vibronic levels of the CCN radical are classified by $K = |\Lambda + l|$ and $P = |\Lambda + l + \Sigma|$, where Λ, l, and Σ are the projections of the electronic, vibrational, and spin angular momenta, respectively, along the linear axis. For the $^2\Pi$ ground state of CCN, Λ=±1 while l can take on values $\pm v_2$, $\pm(v_2-2)$,…, ±1 or 0 and the value of Σ (not to be confused with Λ=0 electronic states or the vibronic symmetry for $K = 0$) is ±1/2. A given vibronic level can then be described by the quantum numbers (v_1,v_2,v_3), K, and P. In addition to the parity label for $K = 0$ (Σ^- or Σ^+), for $K >$ 0 the vibronic levels come in pairs and the lower and upper of these are typically labeled by μ

and κ, respectively. Table V gives the calculated ro-vibronic levels up to 2500 cm^{-1} above the ground state for $K \leq 3$ (Σ, Π, Δ, and Φ) with the total angular momentum J set to the lowest allowed value for each level ($J = P$). This ro-vibronic level structure is also shown graphically in Fig. 4. Table VI compares some selected ro-vibronic transition energies (a full set is available on request) calculated in this work with experiment. Overall the agreement is excellent – both the (100) and (010) bands are reproduced to within 2 cm^{-1} and the spin-orbit splitting in the ground state is underestimated by just under 2 cm^{-1} as well. It should be stressed that no empirical corrections have been made to the *ab initio* PES to obtain this level of agreement. Separate calculations were also carried out where the SO matrix elements between the $^2\Pi$ and $^4\Sigma^-$ states were set to zero. At least for the low-lying transitions shown in Table VI, the neglect of interactions with the $^4\Sigma^-$ state leads to negligible changes, i.e., < 0.02 cm^{-1}.

2. Pure rotational and ro-vibronic intensities

The equilibrium dipole moment in the $X^2\Pi$ electronic ground state of CCN is calculated at the CCSD(T)/aug-cc-pVTZ level to be –0.303 D (see Table S3). The value in the vibrational ground state is calculated to be only slightly smaller in magnitude at -0.299 D. This is about 0.1 D smaller in magnitude than the MRD-CI result calculated previously by Pd and Chandra[3] and 0.3 D smaller than that of Yamashita and Morokuma.[68] Due to the more extensive electron correlation and a basis set that included diffuse functions in the present work, the current value should be the most accurate to date. The present value is actually in surprisingly good agreement with the early small basis set UHF result of Pauzat *et al*.[2] (–0.26 D).

Using the CCSD(T) $^2A'$ and $^2A''$ dipole moment functions of Table S3, accurate integrated ro-vibronic line intensities (in cm/molecule at 300 K) were calculated using the variational ro-vibronic wavefunctions via[69]

$$I(\omega_{if}) = \frac{8\pi^3 N_A \omega_{if} g_i \left[e^{-E_i/kT} - e^{-E_f/kT} \right]}{3hcQ} S(f-i) \qquad (6)$$

where g_i is the total degeneracy of initial state i and the partition function Q is given by

$$Q = \sum_m g_m (2J_m + 1) e^{-E_m/kT}$$

The line strength for spin-dependent interactions was calculated as[70]

$$S(f-i) = (2J+1)(2J'+1)\left| \sum_{I'IN'NK'Ki'i\mu} (-1)^{N'} \sqrt{2N+1} \begin{Bmatrix} N & S & J \\ J' & 1 & N' \end{Bmatrix} C_{NK1\mu}^{N'K'} \bar{\mu}_{\mu}^{I'i'Ii} \right|^2$$

where $\bar{\mu}_{\mu}$ are the dipole moment matrix elements in the molecular frame with $\bar{\mu}_0 = \bar{\mu}_z$ and $\bar{\mu}_{\pm 1} = \mp \frac{1}{\sqrt{2}} \left(\bar{\mu}_x \pm i \bar{\mu}_y \right)$. Integrated vibronic band intensities (in cm^{-2} atm^{-1} at 300 K, which equals 0.40876 x 10^{-19} cm/molecule) were then obtained by two different methods, (a) direct summation of the individual line intensities given by Eq. (6) and (b) a more approximate evaluation using pure vibronic wavefunctions with dipole moments in an Eckart frame embedding.[71] In the latter case g_i is then just the vibronic degeneracy (1 for Σ states and 2 for $K > 0$), $S_{f\text{-}i}$ is the transition strength (sum of squares of vibronic transition dipole matrix elements), and the partition function is given by $Q = \sum_m g_m e^{-E_m/kT}$. It should be noted that Eq. (6) reverts to the relation commonly used by Carter, Rosmus, and co-workers[72] if it is assumed that $\omega_{if} >> kT$ (where the numerical factors at 300 K total 10.182 for cm^{-2} atm^{-1}) For the low frequency bending modes of this work, however, that is not the case and the full partition function must be used.

In the direct summation scheme unfortunately even at 300 K relatively large values of J contribute to each band, e.g., see Figure 4 which displays the calculated rotational structure of the (100) band. This band consists of a main series with ΔΩ=0 and a weaker series corresponding to ΔΩ =1. At these high J values definitive assignments became difficult, due in part to a transition between Hund's cases (a) and (b) (spin-orbit becomes comparable to rotation) and K also becomes less of a good quantum number. In the end the identification was done by visual inspection of wavefunction plots up to as high as J=101/2. The contribution to the integrated band intensity due to all higher J beyond some J_{max} within a given band was then accurately obtained by extrapolation since it was observed that the latter quantity varied as $e^{-aJ_{max}^2}$. The accuracy of this approach was tested in a few cases, e.g., the (100) band, where relatively high J assignments could actually be made. The band intensities calculated in this manner for several selected cases are shown in Table VII. In each case these intensities are also compared to those calculated from pure vibronic transition dipole moments. In each case the agreement between the two approaches is excellent with differences. Not surprisingly the largest differences are observed for the very weak bands, e.g., the (200) overtone, where the two integrated intensities differ by 25%. For the more intense bands the differences, however, are just 1–4%.

Also shown in Table VII are some theoretical band origins compared to experiment. These calculated band origins were obtained from the line positions of the ro-vibronic levels by removing both spin-orbit and rotational terms, i.e., the result of just diagonalizing the operator $\hat{K}_K + V$ (see, Sec. IIB above). The differences between theory and experiment are within 3 cm^{-1} in each case. Unfortunately the comparison is a bit ambiguous since the experimental band origins are dependent on the terms used in the spectroscopic Hamiltonian for the fits over the measured line positions. The accuracy of the present work is better judged by the comparisons made between individual lines as discussed above. In regards to the intensities, clearly the ν_1 stretching fundamental (see also Fig. 5) is the most intense band with the ν_3 stretch about 35% weaker. This is in good agreement with the previous harmonic results of Martin *et al.*[16] Intensities of Renner-Teller subbands are shown in Table VII for the (010) fundamental, as well as the (100) $\rightarrow$ (110) and (010) $\rightarrow$ (110) hot bands. In the latter case the present calculations are able to explain the difficulties in observing the $\kappa\Sigma^+$ state[12]; it is much less intense than the $\mu\Sigma^-$ (by a factor of about 3.5) and there is also strong mixing with the close-lying $\mu\Pi(020)\rightarrow(120)$ band at relatively low *J*, which makes the spin-rotation splittings very irregular. This is identical to what was proposed in the experimental work of Beaton *et al.*[12]

D. Thermochemistry of $X^2\Pi_{1/2}$ CCN

The enthalpy of formation at 0 K, $\Delta H_f(0\text{K})$, for $X^2\Pi_{1/2}$ CCN was computed from the final zero-point energy corrected atomization energy (290.9 kcal/mol as calculated from the ΣD_e value shown in Table I of 296.13 kcal/mol) together with spin-orbit corrections for both the molecule (+0.06 kcal/mol) and atoms (–0.14 kcal/mol), i.e., ΣD_0 = 290.8 kcal/mol. This is about 2 kcal/mol larger than the previously computed value by Martin *et al.*[16] Using reference $\Delta H_f(0\text{K})$ values for the atoms[73] (170.024 kcal/mol for C and 112.469 kcal/mol for N), the resulting 0 K enthalpy of formation, 161.7 kcal/mol, is expected to be accurate to within about 0.5 kcal/mol, with the majority of this uncertainty arising from the higher order correlation contributions to the atomization energy.

IV. CONCLUSIONS

Using explicitly correlated CCSD(T) methods together with contributions from extensive MRCI calculations, accurate near-equilibrium potential energy functions have been calculated for the both the $X^2\Pi$ and $a^4\Sigma^-$ electronic states of the CCN radical. Combined with spin-orbit coupling matrix elements, the low-energy portion of the ro-vibronic spectrum of the $^2\Pi$ state has been calculated using variational methods with inclusion of Renner-Teller interactions for the bending mode. The resulting agreement with the available experimental data is excellent, within at least 3 cm^{-1} without recourse to any empirical corrections. The full set of ro-vibronic transitions calculated in this work is available upon request. Integrated absorption intensities have also been determined for a number of vibronic bands based on analytical CCSD(T) dipole moment functions. Last, using a similar methodology that was employed for the potential energy surfaces was utilized in calculations of the atomization energy and heat of formation of CCN. The resulting value for ΔH_f(0K), 161.7 kcal/mol, is expected to be accurate to about 0.5 kcal/mol.

ACKNOWLEDGMENTS

K.A.P., J.G.H, and K.E.Y. gratefully acknowledge the support of the U.S. National Science Foundation under Grant No. CHE-0723997.

REFERENCES

[1] R. L. Dickman, W. B. Somerville, D. C. B. Whittet, D. McNally, and J. C. Blades, Astrophys. J. Suppl. **53**, 55 (1983); M. Guélin and P. Thaddeus, Astrophys. J. Lett. **212**, L81 (1977).

[2] F. Pauzat, Y. Ellinger, and A. McLean, Astrophys. J. **369**, L13 (1991).

[3] R. Pd and P. Chandra, J. Chem. Phys. **114**, 1589 (2001).

[4] P. Botschwina, M. Horn, J. Flügge, and S. Seeger, J. Chem. Soc. Faraday Trans. **89**, 2219 (1993).

[5] A. M. Mebel and R. I. Kaiser, Astrophys. J. **564**, 787 (2002).

[6] G. W. Fuchs, U. Fuchs, T. F. Giesen, and F. Wyrowski, Astron. Astrophys. **426**, 517 (2004).

[7] D. T. Halfen, D. J. Clouthier, and L. Ziurys, Astrophys. J. **677**, L101 (2008).

[8] A. J. Merer and D. N. Travis, Can. J. Phys. **43**, 1795 (1965).

[9] C. R. Brazier, L. C. O'Brien, and P. F. Bernath, J. Chem. Phys. **86**, 3078 (1987); Y. Ohshima and Y. Endo, J. Mol. Spectrosc. **172**, 225 (1995); H. Kohguchi, Y. Ohshima, and Y. Endo, J. Chem. Phys. **106**, 5429 (1997); M. Feher, C. Salud, and J. P. Maier, J Mol Spectrosc **145**, 246 (1991); M. Feher, C. Salud, J. P. Maier, and A. J. Merer, J Mol Spectrosc **150**, 280 (1991); K. Kawaguchi, T. Suzuki, S. Saito, E. Hirota, and T. Kasuya, J Mol Spectrosc **106**, 320 (1984); K. Hakuta, H. Uehara, K. Kawaguchi, T. Suzuki, and T. Kasuya, J. Chem. Phys. **79**, 1094 (1983).

[10] N. Oliphant, A. Lee, P. F. Bernath, and C. R. Brazier, J. Chem. Phys. **92**, 2244 (1990).

[11] M. D. Allen, K. M. Evenson, D. A. Gillett, and J. M. Brown, J. Mol. Spectrosc. **201**, 18 (2000).

[12] S. A. Beaton, D. A. Gillett, J. M. Brown, M. Feher, and A. Rohrbacher, J. Mol. Spectrosc. **209**, 60 (2001).

[13] K. Hakuta and H. Uehara, J. Chem. Phys. **78**, 6484 (1983).

[14] D. A. Gillett and J. M. Brown, Can. J. Phys. **72**, 1001 (1994).

[15] K. Yamashita and K. Morokuma, Chem. Phys. Lett. **140**, 345 (1987); J. J. Belbruno, Z. C. Tang, R. Smith, and S. Hobday, Mol. Phys. **99**, 957 (2001); J. Wang, Y. Ding, and C. Sun, ChemPhysChem **7**, 710 (2006).

[16] J. M. L. Martin, P. R. Taylor, J. P. Francois, and R. Gijbels, Chem. Phys. Lett. **226**, 475 (1994).

[17] M. Ehara, J. R. Gour, and P. Piecuch, Mol Phys **107**, 871 (2009).

[18] W. Gabriel, E. A. Reinsch, and P. Rosmus, Chem. Phys. Lett. **231**, 13 (1994).

[19] S. Huzinaga, *Gaussian basis sets for molecular calculations*. (Elsevier, Amsterdam, 1984).

[20] P.-O. Widmark, P.-Å. Malmqvist, and B. O. Roos, Theor. Chim. Acta **77**, 291 (1990).

[21] L. Jutier and C. Léonard, Mol. Phys. **105**, 1105 (2007).

[22] E. Garand, T. I. Yacovitch, and D. M. Neumark, J. Chem. Phys. **130**, 064304 (2009).

[23] W. Klopper, F. R. Manby, S. Ten-no, and E. F. Valeev, Int. Rev. Phys. Chem. **25**, 427 (2006); T. Helgaker, W. Klopper, and D. P. Tew, Mol. Phys. **106**, 2107 (2008).

[24] T. B. Adler, G. Knizia, and H.-J. Werner, J. Chem. Phys. **127**, 221106 (2007); G. Knizia, T. B. Adler, and H.-J. Werner, J. Chem. Phys. **130**, 054104 (2009).

[25] MOLPRO, version 2010.1, a package of ab initio programs, H.-J. Werner, P. J. Knowles, R. Lindh, F. R. Manby, M. Schütz *et al.*, see http://www.molpro.net.

[26] S. Ten-no, Chem. Phys. Lett. **398**, 56 (2004).

[27] P. J. Knowles, C. Hampel, and H.-J. Werner, J. Chem. Phys. **99**, 5219 (1993); G. E. Scuseria, Chem. Phys. Lett. **176**, 27 (1991); J. D. Watts, J. Gauss, and R. J. Bartlett, J. Chem. Phys. **98**, 8718 (1993).

[28] K. A. Peterson, T. B. Adler, and H.-J. Werner, J. Chem. Phys. **128**, 084102 (2008).

[29] F. Weigend, Phys. Chem. Chem. Phys. **4**, 4285 (2002).

[30] S. Ten-no and F. R. Manby, J. Chem. Phys. **119**, 5358 (2003); F. R. Manby, J. Chem. Phys. **119**, 4607 (2003).

[31] F. Weigend, A. Köhn, and C. Hättig, J. Chem. Phys. **116**, 3175 (2002).

[32] K. E. Yousaf and K. A. Peterson, J. Chem. Phys. **129**, 184108 (2008).

[33] W. Kutzelnigg, Theor. Chim. Acta **68**, 445 (1985); W. Klopper and C. C. M. Samson, J. Chem. Phys. **116**, 6397 (2002).

[34] E. F. Valeev, Chem. Phys. Lett. **395**, 190 (2004).

[35] H.-J. Werner, T. B. Adler, and F. R. Manby, J. Chem. Phys. **126**, 164102 (2007).

[36] G. Knizia and H.-J. Werner, J. Chem. Phys. **128**, 154103 (2008).

[37] J. G. Hill, K. A. Peterson, G. Knizia, and H.-J. Werner, J. Chem. Phys. **131**, 194105 (2009).

[38] D. W. Schwenke, J. Chem. Phys. **122**, 014107 (2004).

[39] J. G. Hill, S. Mazumder, and K. A. Peterson, J. Chem. Phys. **132**, 054108 (2010).

[40] C. Hättig, Phys. Chem. Chem. Phys. **7**, 59 (2005).

[41] M. Douglas and N. M. Kroll, Ann. Phys. (N.Y.) **82**, 89 (1974); G. Jansen and B. A. Hess, Phys. Rev. A **39**, 6016 (1989).

[42] W. A. de Jong, R. J. Harrison, and D. A. Dixon, J. Chem. Phys. **114**, 48 (2001).

[43] T. H. Dunning Jr, J. Chem. Phys. **90**, 1007 (1989).

[44] D. Feller, K. A. Peterson, and D. A. Dixon, J. Chem. Phys. **129**, 204105 (2008).

[45] A. Karton, E. Rabinovich, J. M. L. Martin, and B. Ruscic, J. Chem. Phys. **125**, 144108 (2006); A. Tajti, P. G. Szalay, A. G. Csaszar, M. Kallay, J. Gauss, E. F. Valeev, B. A. Flowers, J. Vazquez, and J. F. Stanton, J. Chem. Phys. **121**, 11599 (2004).

[46] J. Noga and R. J. Bartlett, J. Chem. Phys. **86**, 7041 (1987); G. E. Scuseria and H. F. Schaefer, Chem. Phys. Lett. **132**, 382 (1988); J. D. Watts and R. J. Bartlett, J. Chem. Phys. **93**, 6104 (1993).

[47] M. Kállay, MRCC, a string-based quantum chemical program suite, Budapest University of Technology and Economics, 2001; M. Kállay and P. R. Surján, J. Chem. Phys. **115**, 2945 (2001).

[48] M. Kállay and P. R. Surján, J. Chem. Phys. **115**, 2945 (2001); S. A. Kucharski and R. J. Bartlett, Theor. Chim. Acta **80**, 387 (1991); S. A. Kucharski and R. J. Bartlett, J. Chem. Phys. **97**, 4282 (1992); N. Oliphant and L. Adamowicz, J. Chem. Phys. **94**, 1229 (1991).

[49] D. Z. Goodson, J. Chem. Phys. **116**, 6948 (2002); D. Feller, K. A. Peterson, and T. D. Crawford, J. Chem. Phys. **124**, 054107 (2006).

[50] T. J. Lee and P. R. Taylor, Int. J. Quantum Chem. Symp. **23**, 199 (1989).

[51] C. L. Janssen and I. M. B. Nielsen, Chem. Phys. Lett. **290**, 423 (1998).

[52] P. J. Knowles and H.-J. Werner, Chem. Phys. Lett. **145**, 514 (1988); H.-J. Werner and P. J. Knowles, J. Chem. Phys. **89**, 5803 (1988).

[53] S. R. Langhoff and E. R. Davidson, Int. J. Quantum Chem. **8**, 61 (1974); J. Simons, J. Phys. Chem. **93**, 626 (1989).

[54] See supplementary material at http://dx.doi.org/??? for tables S1-S4, which include coefficients of the potential, dipole, and spin-orbit functions. .

[55] I. M. Mills, in *Molecular Spectroscopy: Modern Research*, edited by K. N. Rao and C. W. Mathews (Academic, New York, 1972), Vol. 1; D. Papoušek and M. R. Aliev, *Molecular Vibrational/Rotational Spectra*. (Academia, Prague, 1982).

[56] J. Senekowitsch, Ph.D. thesis, Universität Frankfurt, Frankfurt, Germany, 1988.

[57] R. A. Kendall, T. H. Dunning Jr, and R. J. Harrison, J. Chem. Phys. **96**, 6796 (1992).

[58] A. Berning, M. Schweizer, H.-J. Werner, P. J. Knowles, and P. Palmieri, Mol. Phys. **98**, 1823 (2000).

[59] D. E. Woon and T. H. Dunning Jr, J. Chem. Phys. **103**, 4572 (1995).

[60] A. Nicklass, K. A. Peterson, A. Berning, H.-J. Werner, and P. J. Knowles, J. Chem. Phys. **112**, 5624 (2000).

[61] A. Mitrushchenkov, to be published.

[62] B. T. Sutcliffe and J. Tennyson, Int. J. Quantum Chem. **39**, 183 (1991).

[63] S. Carter and N. C. Handy, Mol Phys **52**, 1367 (1984).

[64] A. S. Dickinson and P. R. Certain, J. Chem. Phys. **49**, 4209 (1968); D. O. Harris, G. G. Engerholm, and W. D. Gwinn, J. Chem. Phys. **43**, 1515 (1965); J. C. Light and T. Carrington, Adv. Chem. Phys. **114**, 263 (2000).

[65] R. Barrett, M. Berry, T. Chan, J. Demmel, J. Donato, J. Dongarra, V. Eijkhout, R. Pozo, C. Romine, and H. A. Van der Vorst, in *Templates for the solution of linear systems: building blocks for iterative methods* (SIAM, Philadelphia, 1994); G. L. Sleijpen and H. A. Van der Vorst, SIAM J. Matrix Anal. Appl. **172**, 401 (1996).

[66] P. F. Bernath, *Spectra of Atoms and Molecules*, 2nd ed. (Oxford University Press, New York, 2005).

[67] K. A. Peterson, A. Mitrushchenkov, and J. S. Francisco, Chem. Phys. **346**, 34 (2008).

[68] K. Yamashita and K. Morokuma, Chem. Phys. Lett. **140**, 345 (1987).

[69] M. A. H. Smith, C. P. Rinsland, B. Fridovich, and K. N. Rao, in *Molecular Spectroscopy: Modern Research*, edited by K. N. Rao (Academic Press, Orlando, FL, 1985).

[70] C. R. Le Sueur, S. Miller, J. Tennyson, and B. T. Sutcliffe, Mol. Phys. **76**, 1147 (1992).

[71] C. Eckart, Phys. Rev. **47**, 552 (1935).

[72] J. Senekowitsch, S. Carter, A. Zilch, H.-J. Werner, N. C. Handy, and P. Rosmus, J. Chem. Phys. **90**, 783 (1989).

[73] W. R. Stevens, B. Ruscic, and T. Baer, J. Phys. Chem. A **114**, 13134 (2010).

Table I. Convergence of CCSD(T)-F12b equilibrium geometries (Å), anharmonic frequencies (ν_i in cm^{-1}, from SURFIT), and equilibrium atomization energies (ΣD_e, in kcal/mol) for the $\tilde{X}\,^2\Pi$ CCN radical.[a] The average of the $^2A'$ and $^2A''$ potential energy surfaces was employed.

	$r_{C\text{-}C}$	$r_{C\text{-}N}$	ν_1	ν_2[k]	ν_3	ΣD_e
VDZ-F12	1.3825	1.1857	1923.4	320.6	1033.4	288.74
VTZ-F12	1.3808	1.1849	1930.3	321.8	1038.5	292.51
VQZ-F12	1.3805	1.1846	1932.3	322.7	1039.1	293.28
CBS[a]	1.3804	1.1846	1932.5	323.1	1039.3	293.68
+ΔCV[b]	1.3766	1.1820	1942.2	325.8	1045.7	295.40
+ΔDK[c]	1.3764	1.1818	1941.4	325.7	1045.2	295.15
+ΔMRCI+Q[d]	1.3749	1.1847	1923.3	322.3	1050.4	
Expt.[e]			1923.3		1050.8	
Alternative ΔHC:						
CBS+ΔCV+ΔDK+ΔT[f]	1.3764	1.1813	1947.1	325.6	1047.3	294.73
+ΔQ[g]	1.3753	1.1836	1931.2	323.5	1049.6	295.97
+ΔQ +ΔFCI(cf)[h]	1.3752	1.1840	1928.0	323.2	1050.0	296.13
+ΔQ +ΔFCI(cf, corr)[h]	1.3743	1.1857	1911.4	321.0	1051.8	296.94
ΔHC summary						
ΔCC[i]	-0.0012	+0.0022	-13.4	-2.5	+4.8	+0.98
ΔMRCI[j]	-0.0008	+0.0017	-11.4	-1.7	+4.1	
ΔMRCI+Q[j]	-0.0015	+0.0029	-18.1	-3.4	+5.2	

[a] The CBS limit was obtained by extrapolating the VTZ-F12 and VQZ-F12 correlation energies using Eq. (2).

[b] CCSD(T)/CBS plus the contribution of correlating the 1*s* electrons at the CCSD(T)-F12b/cc-pCVTZ-F12 level of theory.

[c] CCSD(T)/CBS +ΔCV plus a scalar relativistic correction from the conventional CCSD(T)/cc-pVTZ(-DK) level of theory.

[d] CCSD(T)/CBS +ΔCV + ΔDK with a higher level correlation contribution define by MRCI+Q – CCSD(T) with the cc-pVTZ basis set.

[e] Ref. 10

[f] Includes a CCSDT – CCSD(T) correction with the cc-pVTZ basis set.

[g] Includes a CCSDTQ – CCSDT correction with the cc-pVDZ basis set.

[h] ΔFCI(cf) results include a continued fraction extrapolation as detailed in Eq. (3). ΔFCI(cf, corr) replaces the CCSD total energy in Eq. (3) by its correlation energy.

[i] Total higher order coupled cluster correlation correction, i.e., ΔT+ΔQ+ΔFCI(cf).

[j] The difference between CAS-MRCI or CAS-MRCI+Q and CCSD(T) calculations, each with the cc-pVTZ basis set.

[k] Assuming J=1 without inclusion of Renner-Teller couplings.

Table II. Spectroscopic constants of $X^2\Pi$ CCN derived from the final composite CBS+ΔCV+ΔDK+ΔMRCI+Q potential energy functions using 2nd-order vibrational perturbation theory. The average values were obtained from a mean $^2A'$ and $^2A''$ potential energy function.

Constant	Average	$^2A''$	$^2A'$
r_e (CC) (Å)	1.3749	1.3749	1.3749
r_e (CN) (Å)	1.1847	1.1847	1.1847
B_e (MHz)	11,937.2	11937.2	11937.2
B_0 (MHz)	11,924	11,955	11,907
α_1 (MHz)	78.3	78.5	78.0
α_2 (MHz)	-62.3	-93.5	-45.2
α_3 (MHz)	72.4	72.7	72.2
D_e (KHz)	6.22	6.22	6.22
q_e (MHz)	33.75	42.18	29.87
ω_1 (cm^{-1})	1967.2	1967.2	1967.3
ω_2 (cm^{-1})	322.2	243.5	385.1
ω_3 (cm^{-1})	1058.3	1058.2	1058.3
X_{11} (cm^{-1})	-13.3	-13.3	-13.3
X_{12} (cm^{-1})	-7.9	-7.6	-8.3
X_{13} (cm^{-1})	-19.1	-19.2	-19.1
X_{22} (cm^{-1})	-0.5	-0.3	-0.9
X_{23} (cm^{-1})	7.0	10.7	5.4
X_{33} (cm^{-1})	-2.6	-2.6	-2.6
X_{ll} (cm^{-1})	1.62	1.51	1.83
ε [a]	0.429		
$\varepsilon\omega_2$ (cm^{-1})	138.1		
ν_1 (cm^{-1})	1923.3	1923.4	1922.8
ν_2 (cm^{-1}) [b]	322.3	246.1	383.3
ν_3 (cm^{-1})	1050.4	1054.1	1048.9
$G(000)$ (cm^{-1})	1825.2	1748.7	1886.8

[a] The Renner parameter, $\varepsilon = \frac{\omega_{2,A'}^2 - \omega_{2,A''}^2}{\omega_{2,A'}^2 + \omega_{2,A''}^2}$.

[b] Assuming J=1 without inclusion of Renner-Teller couplings.

Table III. Convergence of CCSD(T)-F12b equilibrium geometries, (Å) anharmonic frequencies (ν_i in cm^{-1}, from SURFIT), and adiabatic excitation energy T_0 (in cm^{-1}) for the $a^4\Sigma^-$ excited state of the CCN radical.[a]

	$r_{C\text{-}C}$	$r_{C\text{-}N}$	ν_1	ν_2[b]	ν_3	T_0
VDZ-F12	1.3295	1.1914	1768.4	436.6	1162.0	8231
VTZ-F12	1.3285	1.1906	1777.1	438.5	1165.2	8360
VQZ-F12	1.3281	1.1902	1779.5	439.7	1165.9	8373
CBS	1.3279	1.1902	1779.3	440.2	1166.4	8385
+ΔCV	1.3247	1.1876	1786.3	443.2	1171.9	8224
+ΔDK	1.3245	1.1875	1785.1	443.1	1171.7	8274
+ΔMRCI+Q	1.3233	1.1905	1771.8	439.4	1175.4	8544
Alternative ΔHC:						
CBS+ΔCV+ΔDK+ΔT	1.3247	1.1876	1799.0	443.3	1174.1	8255
+ΔQ	1.3241	1.1895	1783.0	440.6	1173.7	8339
+ΔFCI(cf)	1.3240	1.1898	1779.9	440.1	1173.5	8351
ΔHC summary						
ΔCC	-0.0005	+0.0023	-5.2	-3.0	+1.8	+77
ΔMRCI	+0.0011	+0.0007	+6.0	-2.1	+0.7	-417
ΔMRCI+Q	-0.0012	+0.0030	-13.3	-3.7	+3.7	+270

[a] See footnotes to Table I.

[b] Assuming J=1.

Table IV. Spectroscopic constants of the $a^4\Sigma^-$ excited state of CCN derived from the CBS+ΔCV+ΔDK+ΔMRCI+Q composite potential energy function using 2nd-order vibrational perturbation theory.

Constant		Constant	
T_0 (cm^{-1})	8544	ω_1 (cm^{-1})	1821.8
r_e (CC) (Å)	1.3233	ω_2 (cm^{-1})	443.2
r_e (CN) (Å)	1.1905	ω_3 (cm^{-1})	1178.5
B_e (MHz)	12373.4	X_{11} (cm^{-1})	-21.5
B_0 (MHz)		X_{13} (cm^{-1})	4.6
α_1 (MHz)	77.2	X_{33} (cm^{-1})	-6.0
α_2 (MHz)	-39.2	X_{12} (cm^{-1})	-9.2
α_3 (MHz)	61.8	X_{23} (cm^{-1})	6.6
D_e (KHz)	5.69	X_{22} (cm^{-1})	-1.7
q_e (MHz)	29.85	X_{ll} (cm^{-1})	2.19
		ν_1 (cm^{-1})	1771.8
		ν_2 (cm^{-1})[a]	439.4
		ν_3 (cm^{-1})	1175.4
		$G(000)$ (cm^{-1})	1934.6

[a] Assuming J=1.

Table V. Calculated ro-vibronic energies (J=P) for low-lying states ($v_1v_2v_3$) of $\tilde{X}^2\Pi$ CCN (in cm^{-1}).

$^2\Sigma^-$		$^2\Sigma^+$		$^2\Delta_{3/2}$		$^2\Delta_{5/2}$	
(010)	200.99	(010)	478.76	(010)	295.26	(010)	329.52
(030)	687.98	(030)	1236.63	(030)μ	727.67	(030)μ	738.21
(050)	1170.71	(011)	1583.73	(050)μ	1175.69	(050)μ	1157.94
(011)	1263.58	(050)	1987.48	(030)κ	1234.01	(030)κ	1249.72
(070)	1654.10	(031)	2298.70	(011)	1357.41	(011)	1391.66
(031)	1767.05	(110)	2395.32	(070)μ	1672.89	(070)μ	1673.69
(110)	2117.51	(012)	2578.11	(031)μ	1805.02	(031)μ	1815.15
(090)	2135.38	(070)	2735.89	(050)κ	1977.69	(050)κ	1972.10
(051)	2262.92			(090)μ	2153.50	(090)μ	2159.95
(012)	2317.71			(110)	2212.85	(110)	2247.67
(130)	2595.07			(051)μ	2253.71	(051)μ	2234.10
(0,11,0)	2614.53			(031)κ	2310.08	(031)κ	2328.11
				(012)	2411.64	(012)	2445.59
$^2\Pi_{1/2}$		$^2\Pi_{3/2}$		(0110)μ	2625.53	(0110)μ	2620.65
(000)	0.00	(000)	38.90				
(020)μ	456.33	(020)μ	462.01	$^2\Phi_{5/2}$		$^2\Phi_{7/2}$	
(020)κ	848.92	(020)κ	838.29	(020)	580.31	(020)	609.51
(040)μ	938.73	(040)μ	948.76	(040)μ	1005.62	(040)μ	1020.22
(001)	1052.04	(001)	1090.82	(060)μ	1452.50	(060)μ	1446.14
(060)μ	1418.05	(060)μ	1417.05	(040)κ	1580.85	(040)κ	1585.36
(021)μ	1525.91	(021)μ	1532.18	(021)	1655.67	(021)	1683.65
(040)κ	1610.16	(040)κ	1609.48	(080)μ	1935.50	(080)μ	1941.13
(080)μ	1899.14	(080)μ	1901.77	(041)μ	2089.69	(041)μ	2103.78

(021)κ	1906.83	(021)κ	1898.45	(060)μ	2333.04	(060)μ	2319.06
(100)	1924.88	(100)	1963.64	(0,10,0)μ	2423.1	(0,10,0)μ	2436.36
(041)μ	2024.52	(041)μ	2032.83	(120)	2491.24	(120)	2520.27
(002)	2097.44	(002)	2136.03	(061)μ	2547.77	(061)μ	2537.91
(060)κ	2358.73	(060)κ	2346.34				
(120)μ	2369.30	(120)μ	2375.03				
(0,10,0)μ	2381.35	(0,10,0)μ	2394.07				
(061)μ	2517.82	(061)μ	2516.15				

Table VI. Comparison of selected ro-vibronic transition energies (in cm^{-1}) between theory and experiment for the $X^2\Pi$ state of CCN.

Transition or Energy difference	This work	Expt.
The (100) band[a]		
(100) $^2\Pi_{1/2} \leftarrow$ (000) $^2\Pi_{1/2}$; $P(9/2)$	1921.29	1919.69
(100) $^2\Pi_{1/2} \leftarrow$ (000) $^2\Pi_{1/2}$; $R(5/2)$	1927.60	1925.99
(100) $^2\Pi_{3/2} \leftarrow$ (000) $^2\Pi_{3/2}$; $P(29/2)$	1912.56	1911.04
(100) $^2\Pi_{3/2} \leftarrow$ (000) $^2\Pi_{3/2}$; $R(9/2)$	1929.08	1927.55
The (010) band[b]		
(010) $\mu^2\Sigma^- \leftarrow$ (000) $^2\Pi_{1/2}$; $Q(1/2)$	200.99	199.06
(010) $\mu^2\Sigma^- \leftarrow$ (000) $^2\Pi_{3/2}$; $P(3/2)$	162.09	158.28
(010) $\kappa^2\Sigma^+ \leftarrow$ (010) $\mu^2\Sigma^-$; $Q(1/2)$	277.77	277.10
(010) $^2\Delta_{3/2} \leftarrow$ (000) $^2\Pi_{1/2}$; $R(1/2)$	295.26	295.42
(020) $^2\Phi_{5/2} \leftarrow$ (000) $^2\Pi_{1/2}$; $S(1/2)$	580.31	579.38
Spin-orbit transitions[b]		
(000) $^2\Pi_{3/2} \leftarrow$ (000) $^2\Pi_{1/2}$; $P(7/2)$	35.00	36.89
(000) $^2\Pi_{3/2} \leftarrow$ (000) $^2\Pi_{1/2}$; $Q(3/2)$	37.72	39.60
(000) $^2\Pi_{3/2} \leftarrow$ (000) $^2\Pi_{1/2}$; $R(19/2)$	46.97	48.82
(010) $^2\Delta_{5/2} \leftarrow$ (010) $^2\Delta_{3/2}$; $Q(5/2)$	32.287	34.44
(020) $^2\Phi_{7/2} \leftarrow$ (020) $^2\Phi_{5/2}$; $Q(21/2)$	27.713	29.80
The $1_0^1 2_1^1$ hot band[c]		
(110)$\mu^2\Sigma^- \leftarrow$ (010)$\mu^2\Sigma^-$; $P(7)$, F_1	1913.4571	1911.3882
$F_2 - F_1$	0.0062	0.0066
(110)$^2\Delta \leftarrow$ (010) $^2\Delta$; $R(17/2)$, F_1	1924.8741	1922.9424
$F_2 - F_1$	0.6589	0.3955

[a] Experimental values from Ref. 14.

[b] Experimental values from Ref. 11.

[c] Experimental values from Ref. 12.

Table VII. Selected fundamental, overtone, and combination band origins (in cm^{-1}) together with integrated absorption intensities (in cm^{-2} atm^{-1} at 300 K).[a]

	Frequency		Intensity	
Transition	Theory	Expt.	S_{vib}[b]	S_{int}[b]
(100) ← (000)	1924.75	1923.253[c]	299.28	288.82
(001) ← (000)	1051.96	1050.764[d]	184.31	185.07
(101) ← (000)	2959.87		2.103	1.673
(200) ← (000)	3824.55		0.543	0.464
(002) ← (000)	2097.25	2094.816[d]	26.98	26.87
$\mu\Sigma^-$(010) ← (000)	184.75		15.27	15.41
$\kappa\Sigma^+$(010) ← (000)	459.74		11.72	
Δ(010) ← (000)	292.37		36.52	36.78
$\mu\Sigma^-$ [(011) ← (010)]	1062.58		38.06	34.17
$\kappa\Sigma^+$ [(011) ← (010)]	1053.52		10.22	
Δ [(011) ← (010)]	1062.10		44.70	44.14
$\mu\Sigma^-$ [(110) ← (010)]	1919.21	1917.116[e]	58.55	58.73
$\kappa\Sigma^+$ [(110) ← (010)]	1916.59		16.23	
Δ [(110) ← (010)]	1917.46	1915.838[e]	68.82	67.70
μΠ [(021) ← (020)]	1070.32		22.04	
κΠ [(021) ← (020)]	1058.99		3.417	
Φ [(021) ← (020)]	1074.73		10.78	
μΠ [(120) ← (020)]	1912.98		32.38	
κΠ [(120) ← (020)]	1909.22		5.376	
Φ [(120) ← (020)]	1910.89		17.02	

[a] The theoretical values correspond to pure vibronic transition energies without rotation or spin-orbit coupling. The experimental values were obtained by fits to effective Hamiltonians and hence differ somewhat in their definition compared to theory.

[b] The integrated intensities denoted by S_{vib} were calculated using an Eckart frame, pure vibronic dipole moment expression. See Ref. 70. The values specified by S_{int} were obtained by direct summation of individual ro-vibronic line intensities. See the text.

[c] Reference 14

[d] Reference 10

[e] Reference 12

FIG 1. Convergence of the CCSD(T)-F12b harmonic frequencies for $\tilde{X}\,^2\Pi$ CCN with basis set size. Values calculated from the extrapolated CBS limit surface are indicated by dashed lines.

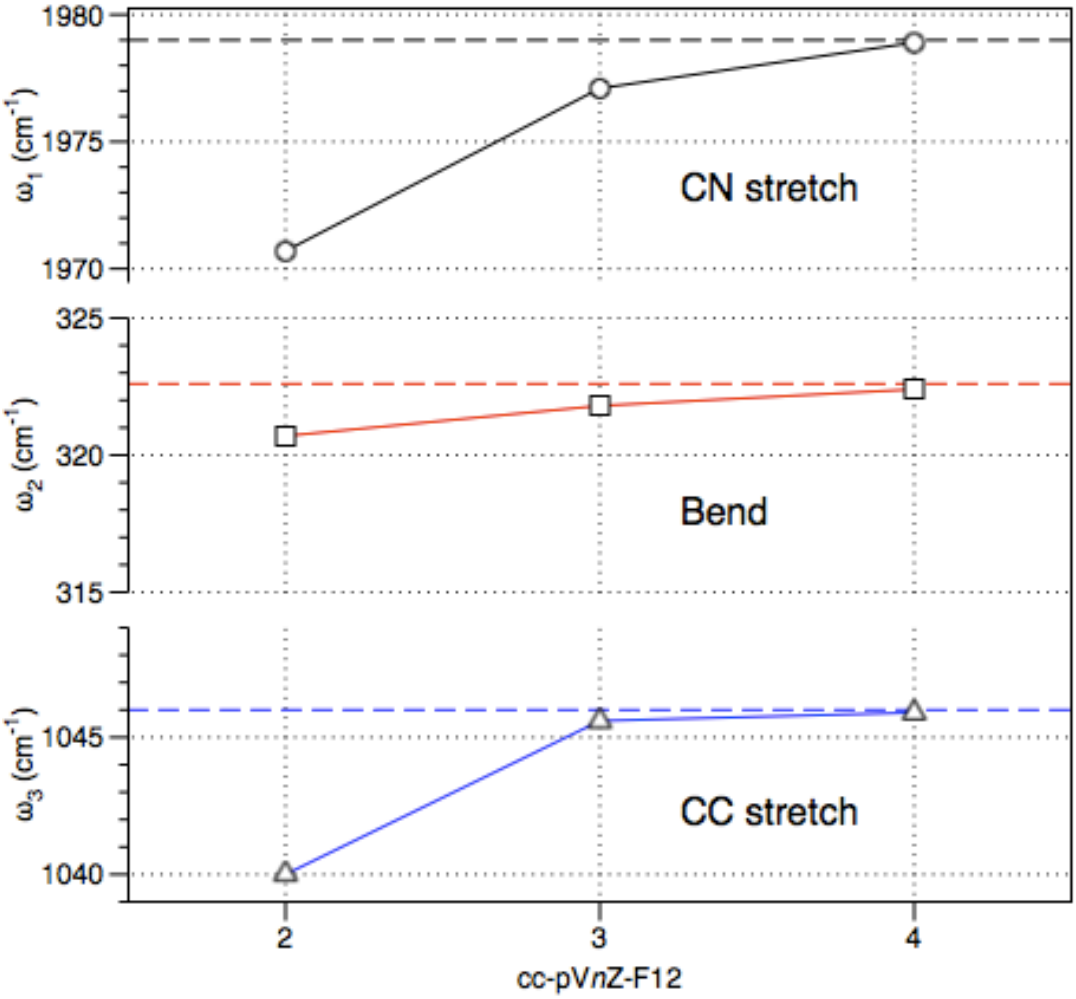

FIG 2. Convergence of the coupled cluster harmonic frequencies for $\tilde{X}\,^2\Pi$ CCN using the cc-pVDZ basis set. The extrapolated FCI(cf) results are denoted with dashed lines.

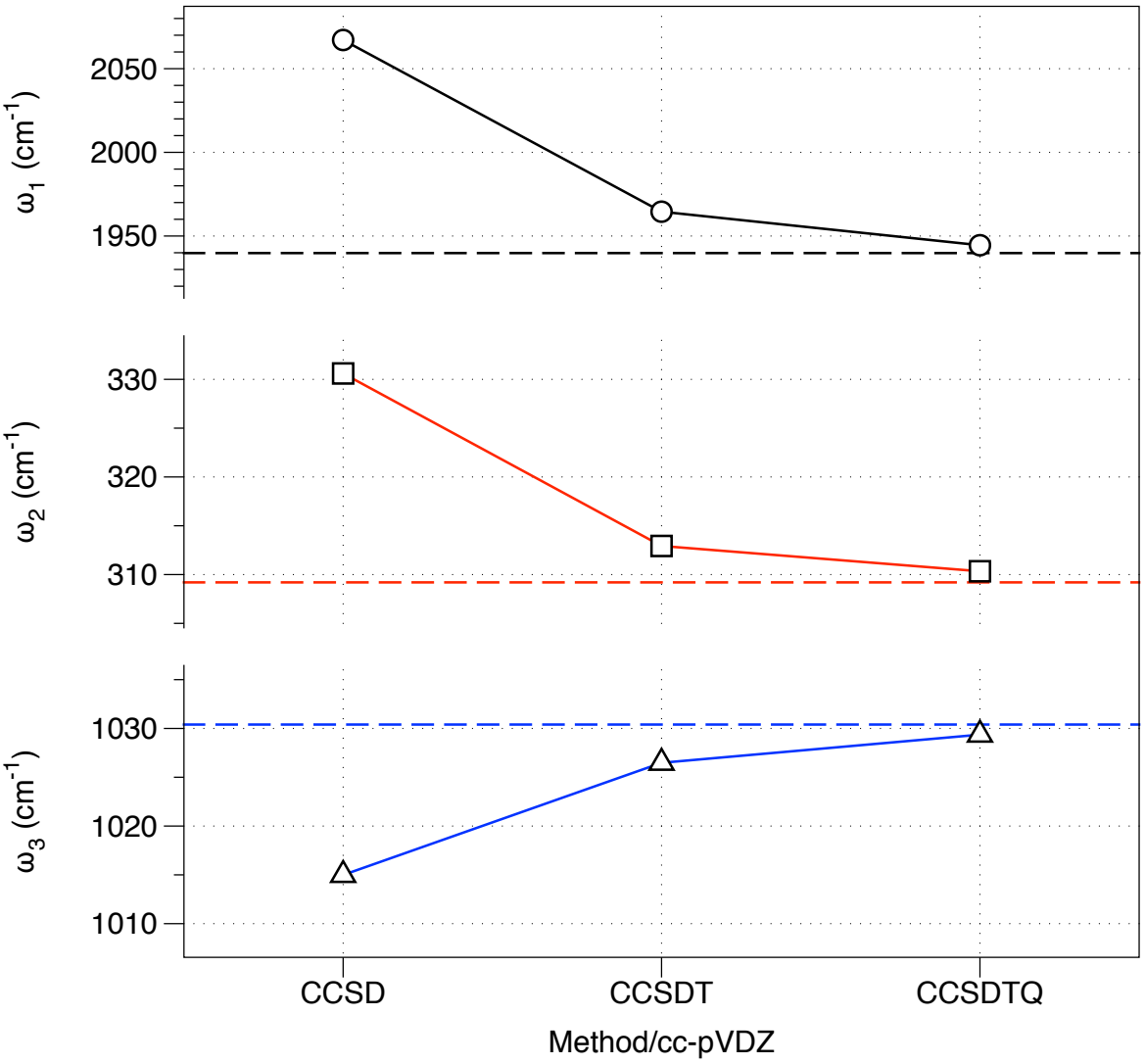

FIG 3. Change in total energy of the ^{2}A′ and ^{2}A″ electronic states of $\tilde{X}\,^2\Pi$ CCN with the bending coordinate from the full composite PES. The bond lengths are fixed at their equilibrium values.

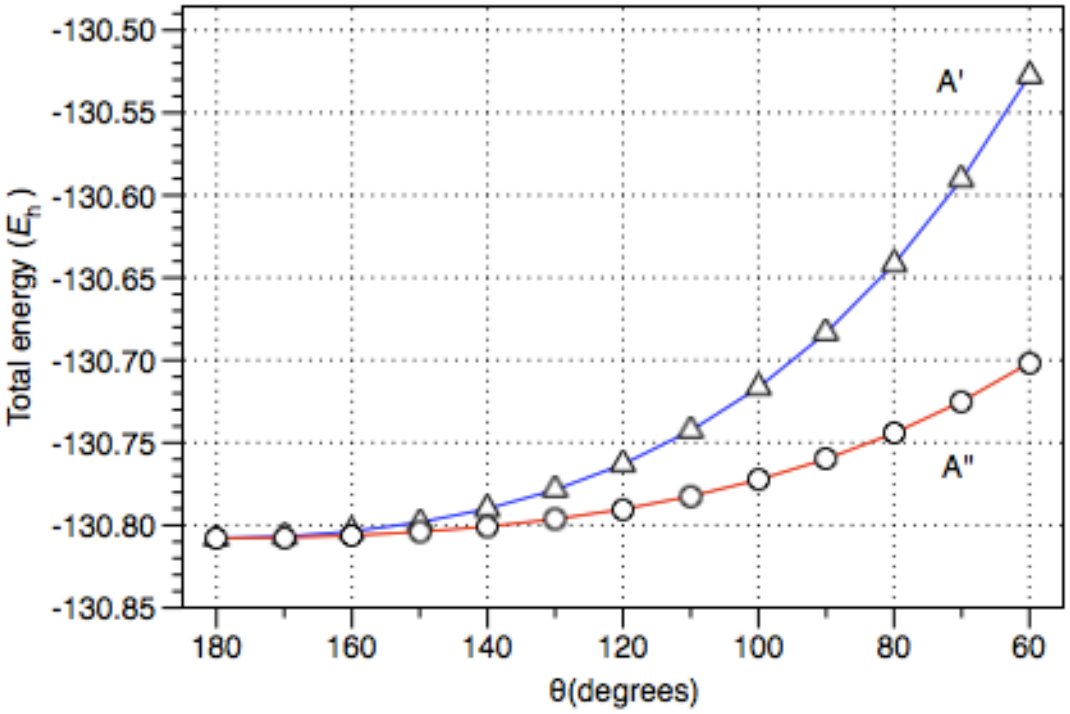

FIG 4. Energy level structure of the ro-vibronic levels (J=P) in the $X^2\Pi$ electronic ground state of CCN.

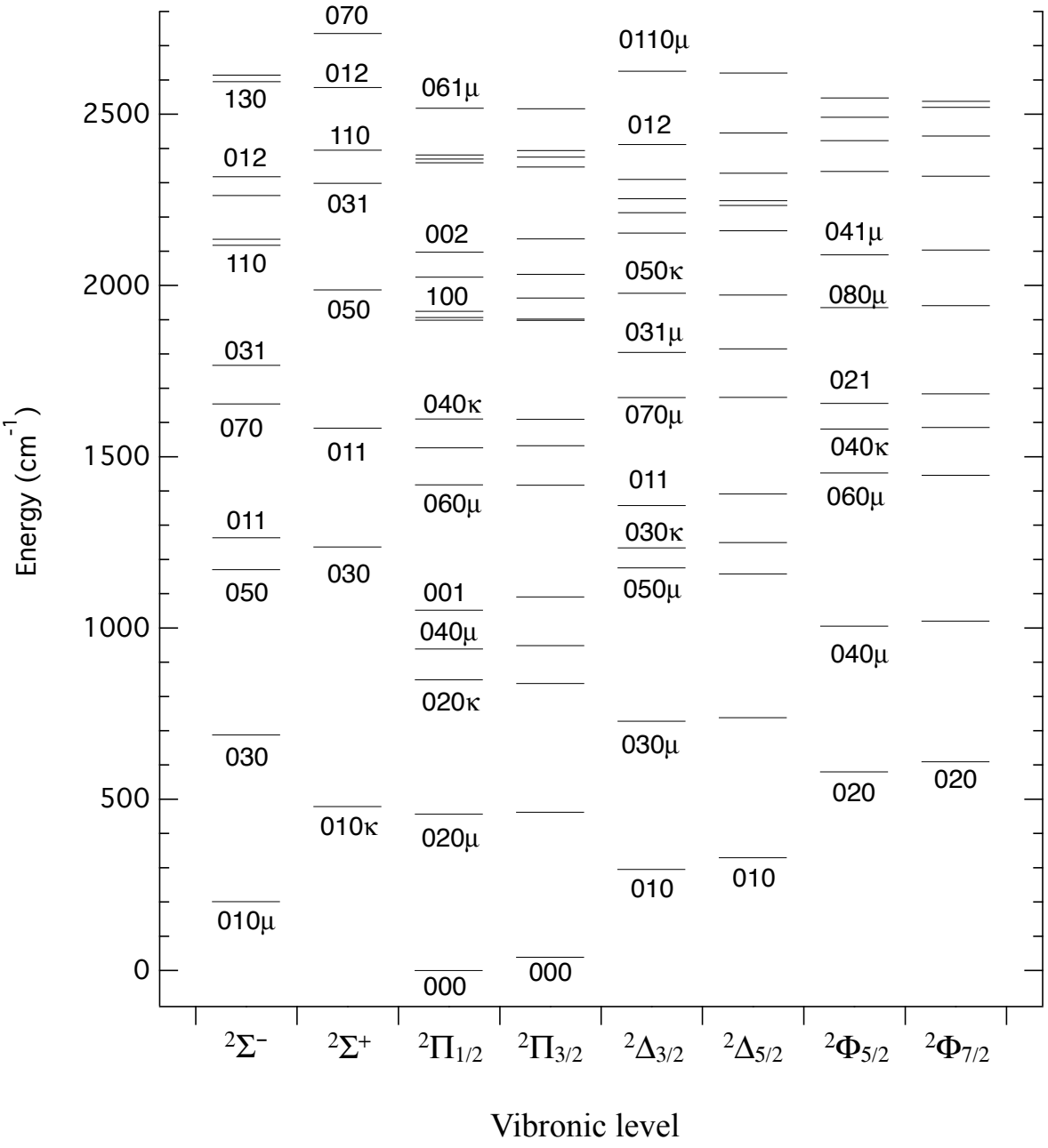

FIG 5. Calculated ro-vibronic structure of the (100) band of CCN at 300 K.